



## Ferromagnetic resonance and low-temperature magnetic tests for biogenic magnetite<sup>☆</sup>

Benjamin P. Weiss<sup>a,b,\*</sup>, Soon Sam Kim<sup>c</sup>, Joseph L. Kirschvink<sup>a</sup>,  
Robert E. Kopp<sup>a</sup>, Mohan Sankaran<sup>d</sup>, Atsuko Kobayashi<sup>e</sup>, Arash Komeili<sup>a</sup>

<sup>a</sup>Division of Geological and Planetary Sciences, California Institute of Technology 170-25, Pasadena, CA 91125, USA

<sup>b</sup>Department of Earth, Atmospheric, and Planetary Sciences, Massachusetts Institute of Technology, Cambridge, MA 02139, USA

<sup>c</sup>Jet Propulsion Laboratory, California Institute of Technology, Pasadena, CA 91125, USA

<sup>d</sup>Division of Chemistry and Chemical Engineering, California Institute of Technology 210-41, Pasadena, CA 91125, USA

<sup>e</sup>Division for Human Life Technology, National Institute of Advanced Industrial Science and Technology (AIST),  
1-8-31 Midorigaoka, Ikeda, Osaka 563-8577, Japan

Received 19 March 2004; received in revised form 15 April 2004; accepted 22 April 2004

### Abstract

Magnetite is both a common inorganic rock-forming mineral and a biogenic product formed by a diversity of organisms. Magnetotactic bacteria produce intracellular magnetites of high purity and crystallinity (magnetosomes) arranged in linear chains of crystals. Magnetosomes and their fossils (magnetofossils) have been identified using transmission electron microscopy (TEM) in sediments dating back to ~ 510–570 Ma, and possibly in 4 Ga carbonates in Martian meteorite ALH84001. We present the results from two rock magnetic analyses—the low-temperature Moskowitz test and ferromagnetic resonance (FMR)—applied to dozens of samples of magnetite and other materials. The magnetites in these samples are of diverse composition, size, shape, and origin: biologically induced (extracellular), biologically controlled (magnetosomes and chiton teeth), magnetofossil, synthetic, and natural inorganic. We confirm that the Moskowitz test is a distinctive indicator for magnetotactic bacteria and provide the first direct experimental evidence that this is accomplished via sensitivity to the magnetosome chain structure. We also demonstrate that the FMR spectra of four different strains of magnetotactic bacteria and a magnetofossil-bearing carbonate have a form distinct from all other samples measured in this study. We suggest that this signature also results from the magnetosomes' unique arrangement in chains. Because FMR can rapidly identify samples with large fractions of intact, isolated magnetosome chains, it could be a powerful tool for identifying magnetofossils in sediments. © 2004 Elsevier B.V. All rights reserved.

**Keywords:** biogenic magnetite; Moskowitz test; ferromagnetic resonance; magnetotactic bacteria

<sup>☆</sup> Supplementary data associated with this article can be found in the online version at doi: 10.1016/j.epsl.2004.04.024.

\* Corresponding author. Division of Geological and Planetary Sciences, California Institute of Technology 170-25, Pasadena, CA 91125, USA. Tel.: +1-626-395-6187; fax: +1-626-568-0935.

E-mail addresses: [bweiss@gps.caltech.edu](mailto:bweiss@gps.caltech.edu) (B.P. Weiss), [soonsam.kim@jpl.nasa.gov](mailto:soonsam.kim@jpl.nasa.gov) (S. Sam Kim), [kirschvink@caltech.edu](mailto:kirschvink@caltech.edu) (J.L. Kirschvink), [rkopp@caltech.edu](mailto:rkopp@caltech.edu) (R.E. Kopp), [mohan@its.caltech.edu](mailto:mohan@its.caltech.edu) (M. Sankaran), [komeili@gps.caltech.edu](mailto:komeili@gps.caltech.edu) (A. Komeili).

## 1. Introduction

Intracellular biomineralization of magnetite is a biochemical process used by bacteria, protists, and animals. Its fossil remains have been reported in sediments as old as the  $\sim 510$ – $570$  Ma Nama Group [1] and tentatively identified in the  $\sim 1.9$  Ga Gunflint Chert [1]. Understanding the evolution of magnetotaxis is of great interest for many different reasons. First, magnetotactic bacteria are the most primitive known organisms that produce biominerals under strict genetic control. Thus, their evolution may be intimately tied to the rise of biomineralization in the Proterozoic era. Second, the magnetosome membrane structure is, with the possible exception of the acidocalcisome [2], the only known membrane-bound organelle yet found in prokaryotes, leading some to suggest that magnetotactic bacteria might be the ancestral eukaryote [3]. Thirdly, magnetofossils 4 billion years old, potentially the oldest known fossil of any kind, have also been reported from carbonates in the Martian meteorite ALH84001 [4–7], although this claim remains highly contentious. Although it is clear that magnetite biomineralization is an ancient process, its time of origin and mode of evolution are poorly known because of the extreme paucity of identified pre-Cenozoic fossils.

The magnetofossil record is largely uncharacterized because of the difficulty of identifying these tiny, submicron objects rather than their intrinsic absence in the fossil record. Past techniques for identification of bacterial magnetofossils have relied on the use of particle extraction followed by high-resolution transmission electron microscopy (TEM) of the extracted magnetic subfractions [1,6,7]. Because these techniques are time-consuming and fairly complex, they are not capable of screening large volumes of sediments for magnetofossils. In this study, we present several techniques capable of rapidly identifying magnetofossil-rich samples.

This work focuses on two magnetic methods. The first is the low-temperature field cooling and zero-field cooling method originally developed by Moskowitz et al. [8,9]. This “Moskowitz test” is thought to be sensitive to the presence of magnetosome chain structures like those produced by the magnetotactic bacteria which have unique low-temperature magnetic behavior. The second and central focus of this paper is

ferromagnetic resonance (FMR), which senses the magnetic anisotropy of samples. The goals of this study were to (a) to experimentally verify that the Moskowitz test is sensitive to the chain structure of magnetosomes, and (b) determine whether FMR can provide a robust diagnostic for the presence of magnetofossils in natural samples.

## 2. Samples

A complete list of samples used for this study is given in Tables 1 and 2. Five classes of previously well-characterized samples were analyzed: biologically controlled magnetite, magnetofossil-bearing carbonates, biologically induced magnetite, synthetic oxides, and natural inorganic samples.

### 2.1. Biologically controlled magnetite

Biologically controlled magnetites are biominerals produced under strict genetic control. They are

Table 1  
Summary of Moskowitz test results on all measured samples

Sample	$\delta_{FC}$	$\delta_{ZFC}$	$\delta_{FC}/\delta_{ZFC}$
<i>Biologically controlled magnetite</i>			
AMB-1	0.23	0.04	5.91
Lysed AMB-1	0.58	0.68	0.85
Old MS-1	0.11	0.09	1.15
<i>Magnetofossil-bearing carbonates</i>			
Clino 985'0"	0.30	0.30	1.03
Clino 991'0"	0.15	0.17	0.89
Clino 993'1"	0.21	0.18	1.18
<i>Biologically induced magnetite</i>			
MR-1 <sup>a</sup>	$\sim 1$	$\sim 1$	$\sim 1$
TOR-39	0.22	0.17	1.25
<i>Synthetic magnetite</i>			
Syn Devouard	0.20	0.25	0.79
Syn A	0.22	0.21	1
Syn C	0.23	0.25	0.94
<i>Natural inorganic</i>			
Lambertville plagioclase	0.34	0.20	1.69
Inorganic goethite	0.86	0.84	1.03
Anorthoclase	0.79	0.82	0.96

<sup>a</sup> FC and ZFC curves were nearly identical, but the sample was too weak to be detected with MPMS above  $\sim 90$  K.

highly ordered crystals with only minor nonstoichiometry and sizes confined to an extremely narrow single domain (SD) size distribution ( $\sim 30\text{--}100$  nm) [10]. The biologically controlled magnetites measured in this study were from four different strains of magnetotactic bacteria and from radula of the Polyplacophoran molluscs (the chitons). The **Chiton** teeth, extracted from *Cryptochiton stelleri*, contain polycrystalline three-dimensional magnetostatically interacting assemblages of magnetites [11] used as hardening agent for their major lateral teeth. Our bacterial samples were freeze-dried whole cells of *Magnetospirillum magnetotacticum* **MS-1**, *Magnetospirillum magneticum* **AMB-1**, **MV-1**, and **MC-1**, all of which produce intracellular magnetite chains for navigation but are members of widely divergent phylogenetic lineages [12,13]. We also analysed a sample **Old MS-1**, which was partly oxidized during its 4 years of exposure to air on our laboratory shelf. The magnetosomes MS-1 and AMB-1 are equant while those of MV-1 and MC-1 have an axis of elongation oriented along that of the chain. Although the individual crystals within a given chain are strongly interacting, the magnetosome chains in bacterial cultures do not interact magnetostatically with one another because of the large ( $\sim 1\ \mu\text{m}$ ) size of the cells that surround them.

We also analyzed samples of these bacteria after having lysed (broken apart) their magnetosome chains in two different ways. First, cells were resuspended in a Tris–HCl buffered solution containing SDS (a lysing agent). Our low-temperature rock magnetic experiments (data not shown) later demonstrated that these samples did not undergo a strong Verwey transition, implying that this lysing method oxidized the magnetosome crystals. Following this failure, we made a second attempt to lyse AMB-1 in which we sonicated the cells in a HEPES buffered solution containing a reductant ( $\beta$ -mercaptoethanol) prior to treating the cells with SDS. The Moskowitz test on this **Lysed AMB-1** exhibited a sharp Verwey transition at 106 K, the same temperature as that of the whole cells (Fig. 1b,c), conclusively demonstrating (see Section 3.1) that the lysed magnetosome chains were not oxidized. This is the first time, to our knowledge, that magnetosome chains have been lysed without concomitantly altering the mineralogy of the individual crystals.

## 2.2. Magnetofossil-bearing carbonates

We analyzed three carbonate samples—**Clino 985'0"**, **Clino 993'1"**, and **Clino 991'0"**—from the Clino core drilled through the Great Bahama Bank carbonate platform [14]. The numbering of each sample indicates its original depth in feet (') and inches (") below the mud pit datum (which was 23.6' above the sea level datum). Clino 991'0" was previously studied by McNeill and Kirschvink [15], who found that it contained intact magnetofossil chains using anhysteretic remanent magnetization (ARM) acquisition and direct TEM imaging experiments. ARM data on core sections from these depths [15] suggest that  $\sim 10\%$  of the magnetites in our three samples are in the form of intact, isolated chains.

## 2.3. Biologically induced magnetite

Biologically induced magnetites are extracellularly produced biominerals that do not crystallize under strict genetic control and typically form as a consequence of iron reduction for energy generation. They are usually poorly crystalline, impure, and extremely fine-grained, mostly in the superparamagnetic (SP) size range (diameters  $< 30$  nm), with a few known examples of SD grains. We analyzed the predominantly SP magnetites produced by the dissimilatory iron-reducing bacteria *Geobacter metallireducens* **GS-15** [16], *Shewanella oneidensis* **MR-1** [12], and *Shewanella alga* **NV-1** [17]. We also studied the extracellular SP and SD magnetites from the thermophilic dissimilatory iron-reducing bacterium *Thermoanaerobacter ethanolicus* **TOR-39** [18]. Finally, we analyzed fine-grained magnetites from *Thermoanaerobacter* **X514** [19] and the hyperthermophilic archaeon *Pyrobaculum islandicum* [20]. All of these biologically induced magnetites are densely clumped and are strongly magnetostatically interacting.

## 2.4. Synthetic oxides

Our synthetic magnetites are laboratory-grown aqueous precipitates. **Syn Devouard**, described by Devouard et al. [21], consists of mostly euhedral SD and SP octahedra with a lognormal size distribution extending up to pseudo single domain (PSD) crystal lengths of 170 nm. **Toda 1**, **TMB-100**, **Syn A**, and **Syn**

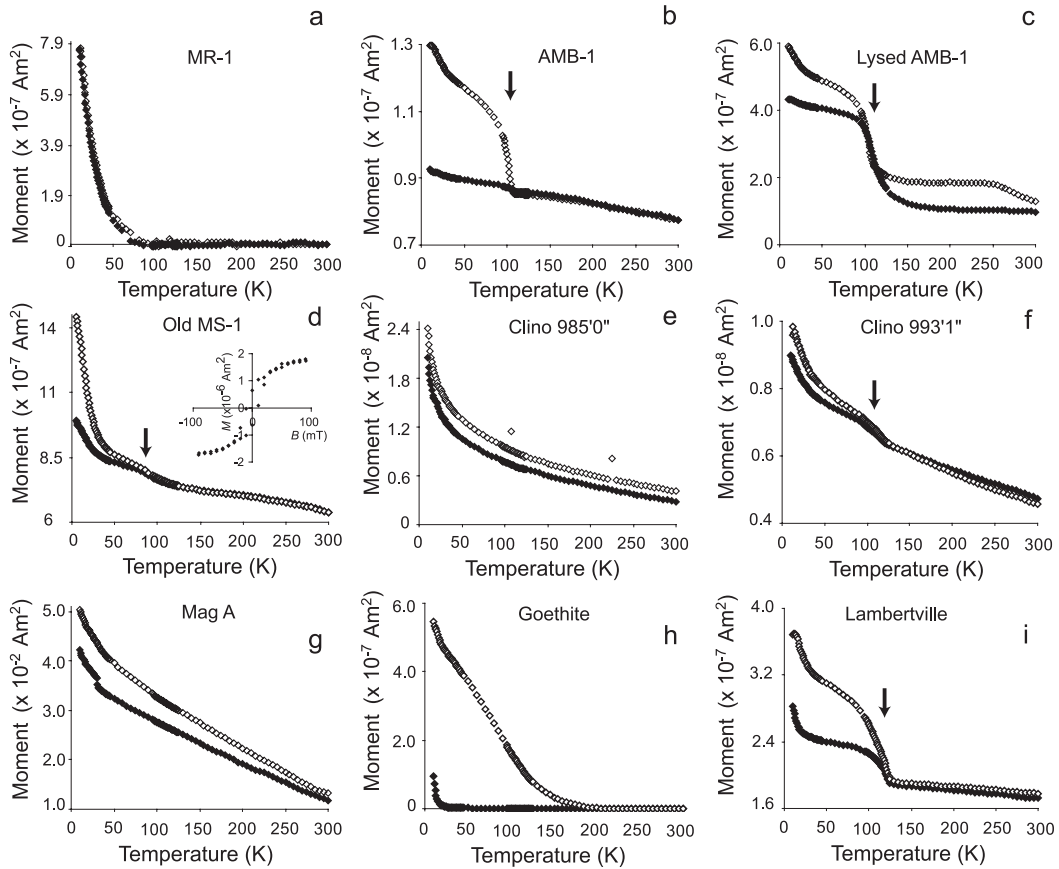


Fig. 1. Results of Moskowitz tests on selected samples. Shown is the moment as a function of temperature as the samples were warming up to room temperature (see text). Open (closed) symbols are field-cool (zero-field-cool) data. The Verwey transitions, estimated from the peak of  $dM/dT$  (see text), are marked with arrows where visible. (a) Superparamagnetic magnetites produced extracellularly by *S. oneidensis* MR-1, (b) whole cells of magnetotactic bacterium *M. magneticum* AMB-1, (c) lysed magnetosome chains from *M. magneticum* AMB-1, (d) oxidized magnetosome chains in Old MS-1 (inset: hysteresis loop at 300 K measured on same sample), magnetofossil-bearing carbonates (e) Clino 985'0'' and (f) Clino 993'1'', (g) synthetic, chemically precipitated magnetite Mag A, (h) Inorganic goethite, and (i) Lambertville plagioclase.

C are magnetostatically interacting magnetites with equant shapes produced by the Toda Industrial company using an undisclosed variant of standard wet methods [22]. Our TEM and field emission scanning electron microscopy (FE-SEM) images (not shown) show that Toda 1 contains SD to PSD ( $\sim 150$ – $200$  nm) magnetites with cubic habit, while TMB-100 and Syn A contain predominantly octahedral crystals of diameter 80–200 and 200–300 nm, respectively, with occasional intergrown masses with diameters of thousands of nanometers. Our FE-SEM images of Syn C show that it is composed of crystals with cubic habit  $\sim 80$  nm in diameter, also occasionally intergrown. These data suggest that Syn A contains pre-

dominantly PSD and multidomain (MD) crystals, while TMB-100 and Syn C contain a mixture of SD, PSD, and MD crystals. This is consistent with our 298 K hysteresis data (not shown) which measured saturation remanence to saturation magnetization ratios for Syn A, TMB-100, and Syn C of  $M_{rs}/M_s = 0.1$ , 0.2, and 0.2, and bulk coercivities of  $H_c = 10$ , 16, and 12 mT, respectively.

We also measured several previously well-characterized powders containing elongate SD crystals: **MO-2230** ( $50 \times 300$  nm maghemite crystals manufactured by Pfizer), **HHO-281** ( $\sim 40 \times 570$  nm maghemite crystals manufactured by Hercules), and **MO-4232** ( $90 \times 600$  nm magnetite crystals manufac-

tured by Pfizer). Finally, we measured two powdered samples of pure, synthetic, acicular SD goethite crystallites (0.25–0.5  $\mu\text{m}$  diameter and with axial ratios of  $\sim 0.1$ ): **Goethite TD** (produced by A. Kappler and T. Daniels) and **Goethite Pfizer** (manufactured by Pfizer). All of our magnetite and maghemite (but not goethite) powders are strongly magnetostatically interacting.

### 2.5. Natural inorganic samples

We studied a variety of natural inorganic mineral and rock powders mainly drawn from hand samples in the Caltech Teaching Collection. Our **Inorganic maghemite**, **Big magnetite**, **Inorganic goethite**, and **Hematite** samples were MD, MD, SD, and SD powders, respectively. We also analyzed an **Ilmenite** powder. Our 298 K hysteresis data (not shown) on the **Anorthoclase** powder measured  $M_{rs}/M_s = 0.09$  and  $H_c = 7$  mT, indicating that it contains predominantly PSD grains. Magnetite was also extracted with a magnet from a **Soil** from Pasadena, CA. The **Lambertville plagioclase** is a mineral separate from the Lambertville diabase containing SD magnetite with uniaxial anisotropy [23]. The **Basalt** sample is from a Hawaii Scientific Drilling Project core through the Kilauea volcano containing predominantly PSD magnetite and titanomagnetite [24].

## 3. Methods

### 3.1. The Moskowitz test and hysteresis loops

The Moskowitz test and hysteresis loops were measured on a wide variety of samples from each of the classes described in Section 2. These data were taken with a Quantum Design Magnetic Property Measurement System (MPMS) housed at the Beckman Institute at Caltech. This instrument is a SQUID gradiometer that measures the moments of  $< \sim 1$   $\text{cm}^3$  samples at temperatures from 1.8 to  $>300$  K while immersed in fields from  $< 0.2$  mT to 5.5 T. Hysteresis loops [25,26], in which the sample's magnetization is measured as a function of applied field, were used to confirm the crystal size and mineralogy of selected samples as a control for interpreting the Moskowitz test and FMR data.

Low-temperature magnetometry permits observations of remanence transitions and changes in magnetization intensity with temperature. Of particular interest is magnetite's  $\sim 125$  K Verwey transition, in which it converts from a high-temperature cubic phase to a low-temperature monoclinic phase. The actual transition temperature is depressed below this value for magnetites with even small amounts of impurities and/or which have been even slightly oxidized. In particular, no Verwey transition will occur for oxidized magnetites with  $\text{Fe}_{3-y}\text{O}_4$  with  $y > 0.035$  or impure magnetites with  $\text{Fe}_{3-x}\text{Z}_x\text{O}_4$  for  $x > 0.039$  for a wide range of impurities  $Z$  including Zn, Ti, Al, Mg, Co, Ni, and Ga [27–29]. In this way, the Verwey transition temperature is a sensitive compositional indicator. Here, we precisely estimated the Verwey transition temperature of each sample from our low-temperature data by determining the temperature at which the derivative of the sample's moment with respect to temperature,  $dM/dT$ , is at a maximum.

In sensing the Verwey transition, the Moskowitz test appears to be a robust indicator of the presence or absence of magnetotactic bacteria [8,30] and also ensures the purity of magnetite in the sample. A series of studies have argued that the test is able to identify these bacteria via its sensitivity both to the magnetosome chain structure [8,9] and also possibly to minor non-stoichiometry of the crystals [30,32], both of which strongly influence the amount of demagnetization that occurs at the Verwey transition.

Following previously described protocols [8], our Moskowitz test consisted of two sets of measurements on each sample: field-cool (FC) and zero-field-cool (ZFC). In both cases, we measured the moment of the sample as it was progressively warmed from 10 to 300 K. FC data were taken after the sample had been previously cooled from 300 K to 10 K in a saturating (5.0 T) field that was then quenched to  $< 0.2$  mT at 10 K. ZFC data were taken after the sample had been previously cooled from 300 to 10 K (after having quenched the magnet at 300 K); before beginning the measurements, this was followed by momentary exposure to a saturating (5.0 T) field at 10 K which was then quenched to  $< 0.2$  mT. The degree to which the FC and ZFC curves diverge below the Verwey transition was quantified by Moskowitz et al. [8] using the ratio  $\delta_{FC}/\delta_{ZFC}$  defined as  $\delta_{FC,ZFC} = [M_{FC,ZFC}(80 \text{ K}) - M_{FC,ZFC}(150 \text{ K})]/M_{FC,ZFC}(80 \text{ K})$  where  $M(T)$

is the moment measured at temperature  $T$  following either FC or ZFC treatment. Empirically, they found that only whole cells of magnetotactic bacteria have  $\delta_{\text{FC}}/\delta_{\text{ZFC}} > 2$ .

### 3.2. Ferromagnetic resonance

Our primary use for FMR is as a sensor of the magnetic anisotropy of ferromagnetic materials. In FMR, a sample is immersed in a DC magnetic field and exposed to microwaves. Due to the Zéeman effect, the sample can absorb this energy with the amount of absorption depending on the strength of the applied and any internal magnetic fields. Despite its maturity as a magnetic technique, FMR has never to our knowledge been used to systematically study the magnetism of microbially mediated ferromagnetic minerals [33]. Our FMR measurements were conducted at X-band (9.3 GHz) with Bruker ESP 300E EPR Spectrometers housed at the Jet Propulsion Laboratory and at Caltech. Most samples were analyzed at both room temperature and again at 77 K. The raw data (Fig. 2) are presented as the derivative of the absorption with respect to magnetic field,  $dI/dB$  (ordinate), as a function of applied field  $B$  (abscissa).

Because of the large number of samples measured in this study, we classified the FMR spectra of each using three parameters: the polycrystalline effective  $g$ -factor,  $g_{\text{eff}}$ , the linewidth ( $\Delta B$  and  $\Delta B_{\text{FWHM}}$ ), and the asymmetry ratio,  $A$  (see Fig. 2a). These FMR parameters and their relationship to the underlying physical properties of the samples are discussed in the Supplementary Information. The linewidth parameters are defined in Fig. 2a. In our definition,  $g_{\text{eff}} = hv/\beta B_{\text{eff}}$ , where  $h$  is Planck's constant,  $v$  is the spectrometer frequency, and  $B_{\text{eff}}$  is the position of the peak of the absorption curve (synonymous with the zero crossing of  $dI/dB$ ; see Fig. 2a). Our asymmetry parameter

is defined as  $A = \Delta B_{\text{high}}/\Delta B_{\text{low}}$ , where  $\Delta B_{\text{high}}$  and  $\Delta B_{\text{low}}$  are defined in Fig. 2a.

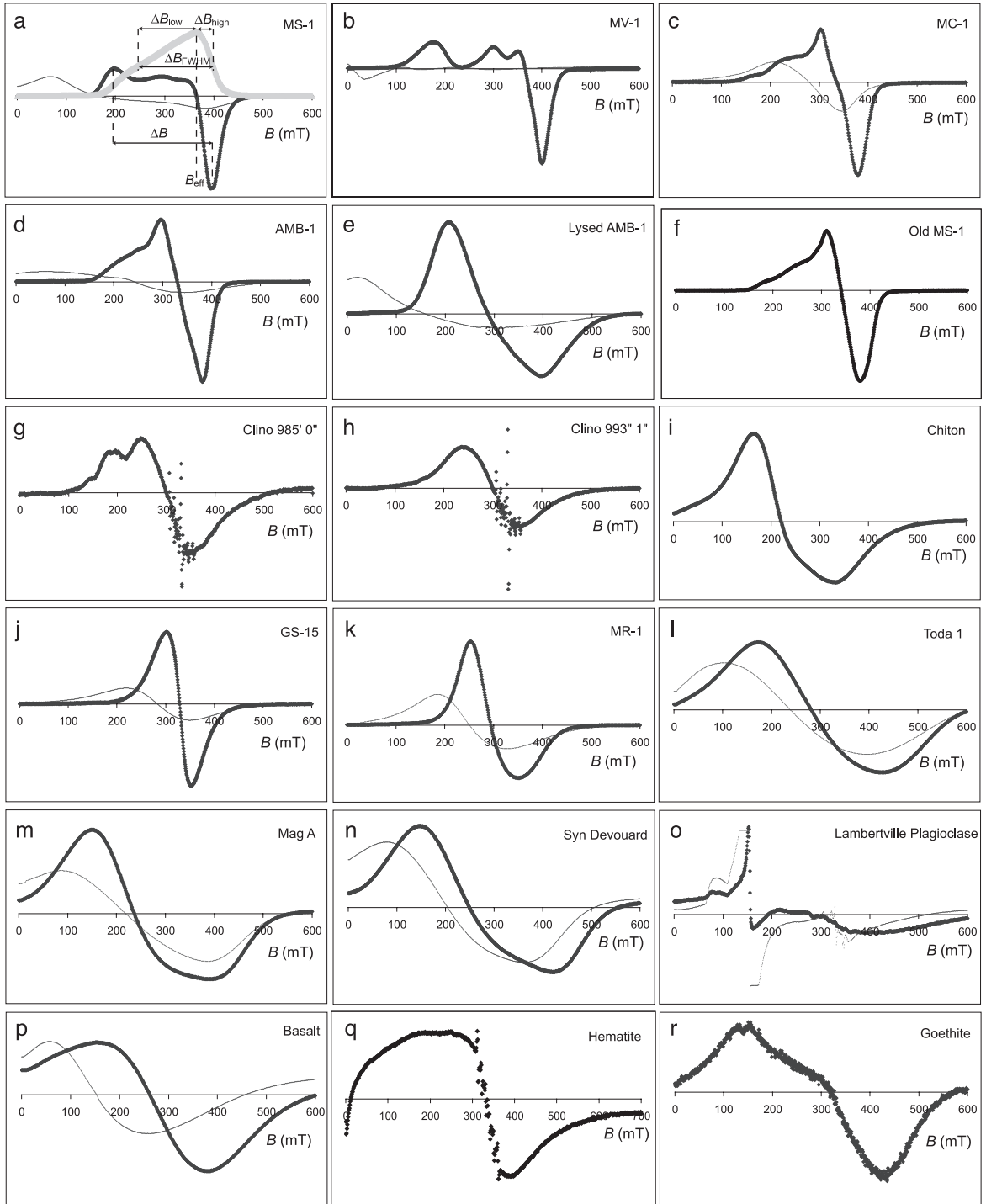
## 4. Results

### 4.1. Moskowitz test

During the course of the Moskowitz tests (Fig. 1), only our SD and larger magnetite-bearing samples exhibited sharp Verwey transitions. That AMB-1's Verwey transition occurs at  $104 \pm 2$  K demonstrates that its magnetosomes are nearly unoxidized (composition  $\text{Fe}_{3-y}\text{O}_4$  for  $y < 0.013$ ) and close to stoichiometric in composition ( $\text{Fe}_{3-x}\text{Z}_x\text{O}_4$  with  $x \leq 0.02 - 0.012$  for a wide range of impurities  $Z$ ) (see Section 3.1). Aside from effects associated with the Verwey transition, all of our magnetite-bearing samples except AMB-1 have FC and ZFC curves that rise steeply with decreasing temperature, indicating that these samples contain varying subfractions of SP grains (diameters of  $\sim < 30$  nm). AMB-1's magnetization curves are relatively flat above and below the Verwey transition (Fig. 1), demonstrating how magnetotactic bacteria produce an unusually restricted SD size distribution of magnetites.

Only intact cells of magnetotactic bacteria strains MS-1, MV-1, and MV-2 strains are known to have  $\delta_{\text{FC}}/\delta_{\text{ZFC}} > 2$  [8]. However, there has yet been no direct experimental proof that this unique feature results from the chain structure rather than from the magnetosomes' other distinctive properties (e.g., their elongate shape, purity, crystallographic perfection, and tight size distribution). Our only sample with  $\delta_{\text{FC}}/\delta_{\text{ZFC}} > 2$  are the AMB-1 whole cells ( $\delta_{\text{FC}}/\delta_{\text{ZFC}} = 5.6$ ), with the next largest being the elongate magnetites of the Lambertville plagioclase (which had  $\delta_{\text{FC}}/\delta_{\text{ZFC}} = 1.7$ , close to a previous measurement on this sample [9]). These features are not shared by the Old MS-1

Fig. 2. Ferromagnetic resonance spectra from selected samples. Shown is the first derivative of the X-band (9.3 GHz) power absorption with respect to the intensity of the applied DC field  $B$ , plotted as a function of  $B$ . Measurements on each sample were taken at both 298 K (bold symbols) and with a few exceptions, again at 77 K (small symbols, when data are available). In (a), we show the absorption (integral of the first derivative data) in bold, light grey symbols, marked with the linewidths  $\Delta B$  and  $\Delta B_{\text{FWHM}}$ , low-field linewidth  $\Delta B_{\text{low}}$ , high-field linewidth  $\Delta B_{\text{high}}$ , and field of peak absorption  $B_{\text{eff}}$ . Samples: magnetotactic bacteria (a) *M. magnetotacticum* MS-1, (b) MV-1, (c) MC-1, (d) *M. magneticum* AMB-1, (e) lysed *M. magneticum* AMB-1 bacterial cells and oxidized magnetosome chains in (f) Old MS-1; (g) magnetofossil-bearing carbonates Clino 985'0" and (h) Clino 993'1" (i) magnetite radula from *C. stelleri*; superparamagnetic magnetites produced extracellularly by (j) *G. metallireducens* GS-15 and (k) *S. oneidensis* MR-1; synthetic, chemically precipitated magnetites (l) Toda 1, (m) Mag A, and (n) Syn Devouard; and natural inorganic samples (o) Lambertville plagioclase, (p) Basalt, (q) Hematite, and (r) Inorganic goethite.



sample, which instead has a soft Verwey transition at 89 K,  $\delta_{FC}/\delta_{ZFC}$  of only 1.1 and  $M_{rs}/M_s = 0.4$  (Fig. 1d), all of which are characteristic of partly maghemitized magnetosome chains (see [8]).

Because the Moskowitz test has never been applied to AMB-1 before, these data provide additional support for the power of the test as an indicator of magnetotactic bacteria. More interestingly, this is also the first application of the Moskowitz test to unoxidized magnetosomes from lysed chains. The  $\delta_{FC}/\delta_{ZFC}$  of the Lysed AMB-1 sample was only 0.85, despite its strong Verwey transition at  $106 \pm 2$  K. This drop in  $\delta_{FC}/\delta_{ZFC}$  following lysing experimentally supports the hypothesis that one of the major reasons the Moskowitz test identifies magnetotactic bacteria is by sensing the alignment of magnetosomes in chains (as opposed to other chemical or crystallographic properties of the individual magnetosomes [30]).

Although the FC and ZFC magnetization curves of *S. oneidensis* MR-1 experienced sharp drops in remanence as the sample warmed up from 10 K, neither curve exhibits an obvious Verwey transition. Both of these features indicate that the sample contains predominantly SP grains, consistent with previous data [12]. The MR-1 FC and ZFC data are very similar to that previously measured on the SP magnetites in GS-15 [8]. The only other sample which showed a strong Verwey transition is the Lambertville plagioclase (discussed above) and the Anorthoclase. The Inorganic Goethite and the synthetic magnetites did not exhibit strong Verwey transitions, had  $\delta_{FC}/\delta_{ZFC} \sim 1$ , and had FC curves lying above their ZFC curves at all temperatures, all properties previously observed for goethites, PSD magnetites, and/or magnetites coated with SP maghemite [34–36].

Among our three Clino samples, only Clino 993'1" showed a Verwey transition (Fig. 1e,f), although other subsamples from these core depths do exhibit the transition (B. Moskowitz, personal communication). The other two Clino samples had FC curves lying above their ZFC curves at all temperatures. Clino 993'1"s transition was not sharp and occurred at 114 K along with a second weaker transition at 95 K, consistent with it containing a mixture of relatively pure magnetite and partially oxidized magnetites. Despite the presence of intact magnetosome chains in all three Clino samples,

they only had  $\delta_{FC}/\delta_{ZFC} = 0.9–1.2$ . In essence, the Moskowitz test was unable to detect the presence of magnetofossils in these samples. The suppressed Verwey transitions and the divergence between the FC and ZFC curves strongly indicate that this failure is probably the result of partial maghemitization of the magnetites in the samples, which has confounded previous attempts [34,37] to use the Moskowitz test as a probe for magnetofossils in natural sediments.

#### 4.2. Ferromagnetic resonance

FMR spectra of fine-particle magnetic materials are influenced by a wide variety of factors, including the sizes of the ferromagnetic crystals, the distance between the ferromagnetic crystals in the sample, mineralogy and composition, crystal habit, and magnetic anisotropy. It is beyond the scope of this paper to discuss all of the details of each of the FMR spectra presented here. Rather, the goal of the present work is to survey a wide variety of samples to determine whether biogenic magnetites have any distinctive FMR properties by which they can be readily identified. As we show below, magnetotactic bacteria, in fact, do have an unusual FMR spectrum that we suggest is a reflection of the magnetosome chain structure.

##### 4.2.1. FMR data: general observations

Selected FMR absorption spectra taken at room temperature and 77 K are presented in Fig. 2, while the FMR parameters measured on all samples are summarized in Fig. 3 and Table 2. Unless explicitly mentioned, our comments below refer to the room-temperature spectra only.

All magnetite-bearing samples have linewidths within the range predicted for magnetite (see Supplementary Information). The biologically induced magnetites as a group have the smallest linewidths,  $g_{\text{eff}}$  closest to the true  $g$ -factor for magnetite (2.12), and the most symmetric lineshapes. Furthermore, their 77 K spectra all have broader linewidths and higher  $g_{\text{eff}}$  than the room-temperature spectra. All of these features are consistent with our expectation that other than TOR-39, the biologically induced samples have extremely small (mostly SP) grain sizes with diameters  $\sim < 30$  nm (see Supplementary Information). Two of these samples—TOR-39 and

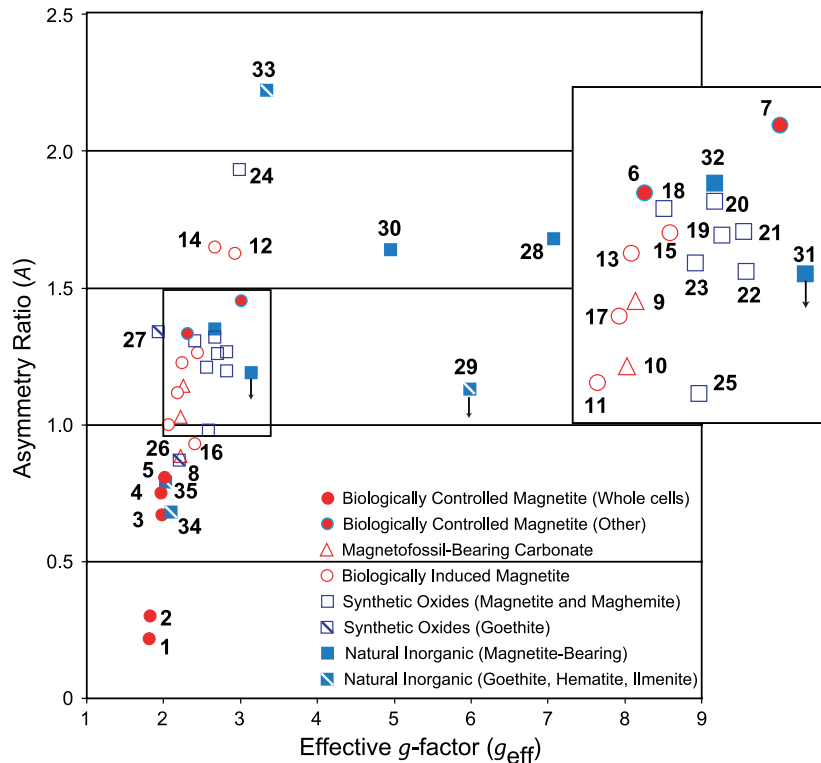


Fig. 3. Summary of room-temperature ferromagnetic resonance spectra from all samples measured. Shown are the asymmetry factor,  $A = \Delta B_{\text{high}} / \Delta B_{\text{low}}$ , plotted as a function of the effective  $g$ -factor,  $g_{\text{eff}}$ .  $\Delta B_{\text{low}}$  and  $\Delta B_{\text{high}}$  are respectively the linewidths on the low-field and high-field side at half of the peak absorption in the integrated spectrum. The field at which peak absorption occurs,  $B_{\text{eff}}$ , is inversely proportional to  $g_{\text{eff}}$ . The boxed region is shown magnified at the upper right. Data used to make this figure are listed in Table 2. Individual samples are: (1) MV-1, (2) *M. magnetotacticum* MS-1, (3) MC-1, (4) *M. magneticum* AMB-1, (5) Old MS-1, (6) Lysed *M. magneticum* AMB-1, (7) magnetite radula from *C. stelleri*; magnetofossil-bearing carbonates (8) Clino 985'0", (9) Clino 991'0", (10) Clino 993'1" biologically induced magnetites produced by (11) *G. metallireducens* GS-15 grown by D. Lovley, (12) *G. metallireducens* GS-15 grown by Vali et al. (in preparation), (13) *S. oneidensis* MR-1, (14) *S. alga* NV-1, (15) *T. ethanolicus* TOR-39, (16) *Thermoanaerobacter* X514, (17) *P. islandicum*; synthetic magnetites and maghemites (18) Toda 1, (19) TMB-100, (20) Syn Devouard, (21) Syn A, (22) Syn C, (23) MO-2230, (24) HHO-281, (25) MO-4232, (26) Goethite Pfizer, (27) Goethite TD; natural inorganic samples (28) Soil magnetite, (29) Ilmenite, (30) Big magnetite, (31) Anorthoclase, (32) Basalt, (33) Inorganic maghemite, (34) Inorganic goethite, (35) Hematite.

MR-1—have linewidths that exceed the magneto-crystalline-anisotropy-determined minimum value for SD magnetite (94 mT; see Supplementary Information), consistent with our expectation that additional broadening should arise from inter-particle magnetostatic interactions.

The powdered and pure polycrystalline samples that have strong saturation magnetizations (the synthetic and natural inorganic magnetites and maghemites, the Chiton, and Lysed AMB-1) as a group have the largest linewidths, most extended highfield absorption (largest  $A$ ) and largest  $g_{\text{eff}}$ . All three of these parameters have values well above those expected for

weakly interacting SD equidimensional samples of magnetite and maghemite (see Supplementary Information). This is a direct manifestation of the strong magnetostatic interactions in these samples which dominate the FMR spectra. For the Inorganic maghemite, an additional factor responsible for these FMR properties are domain effects in the sample's PSD-to-MD-sized crystals [38]. In general, multidomain effects lead to an FMR peak below  $1/3\mu_0 M_s$ , which equals 160 mT for maghemite (see Supplementary Information).

The Lambertville plagioclase is dominated by a sharp resonance at  $g=4.3$  whose intensity varies

inversely with temperature, characteristic of paramagnetic  $\text{Fe}^{3+}$  in plagioclase [39]. This is so intense that it strongly overprints the FMR signature of its exsolved magnetites (which instead control the hysteresis loops). The rest of the natural inorganic magnetite-

Table 2  
Summary of ferromagnetic resonance summary data from all measured samples

Sample	$g_{\text{eff}}$	$\Delta B$ (mT)	$A$
<i>Biologically controlled magnetite</i>			
MS-1	1.82	199	0.30
MV-1	1.82	224	0.22
MC-1	1.98	77	0.67
AMB-1	2.02	84	0.81
AMB-1 lysed	2.31	188	1.33
Old MS-1	1.97	201	0.75
Chiton	3.01	168	1.46
<i>Magnetofossil-bearing carbonates</i>			
Clino 985'0"	2.22	98	0.89
Clino 991'0"	2.26	108	1.14
Clino 993'1"	2.22	112	1.03
<i>Biologically induced magnetite</i>			
GS-15	2.07	54	1.03
MR-1	2.26	98	1.23
NV-1	2.67	89	1.65
TOR-39	2.44	111	1.26
X514	2.40	86	0.93
<i>P. islandicum</i>	2.18	55	1.12
<i>Synthetic oxides</i>			
Toda 1	2.41	253	1.31
TMB 100	2.71	325	1.26
Syn Devourad	2.67	274	1.32
Syn A	2.82	239	1.27
Syn C	2.83	248	1.19
MO-2230	2.57	335	1.21
HHO-281	2.99	273	1.93
MO-4232	2.59	355	0.98
Goethite Pfizer	2.21	68	0.87
Goethite TD	1.94	223	1.34
<i>Natural inorganic</i>			
Soil magnetite <sup>a</sup>	7.08	152	1.68
Ilmenite <sup>b</sup>	5.99	155	<1.13
Big magnetite <sup>a</sup>	4.96	258	1.64
Anorthoclase <sup>b</sup>	3.14	288	<1.19
Basalt <sup>a</sup>	2.67	228	1.35
Inorganic maghemite <sup>a</sup>	3.35	283	2.22
Lambertville plagioclase <sup>c</sup>	–	–	–
Inorganic goethite	2.09	279	0.66
Hematite	2.03	140	0.79

bearing samples (other than the Basalt) have large  $\Delta B$ ,  $g_{\text{eff}} \gg 2$ ,  $A > 1$  (extended high-field absorption), and have high-field minima close to  $1/3\mu_0 M_s$  for magnetite ( $\sim 200$  mT), consistent with the fact that these are MD samples. As expected, our PSD samples—like the Basalt and synthetic magnetites—have  $g_{\text{eff}}$  intermediate between that of these MD samples and the SP biologically induced magnetites.

All of the magnetotactic bacteria (whole cells), the Old MS-1, and one of the magnetofossil-bearing carbonates have room-temperature FMR spectra distinct from all of the rest of our samples. Firstly, they are our only magnetite samples (other than, marginally, X514 and MO-4232) with extended low-field absorption ( $A < 1$ ). Secondly, they are our only samples that show secondary absorption peaks and/or ripple structure on the low field side of the peak absorption. Finally, the magnetotactic bacteria are our only magnetite samples that have  $g_{\text{eff}}$  below 2.12 (while all three of the carbonates have some of the lowest  $g_{\text{eff}}$  among the rest of the sample suite). All three of these properties— $A < 1$ ,  $g_{\text{eff}} < 2.12$ , and secondary low-field absorption peaks—are not expected for SD magnetite dominated by its natural magnetocrystalline anisotropy. This is because room-temperature FMR spectra of SD magnetite crystals have been found to display a spectral asymmetry characteristic of  $K_1 < 0$  [40]. Minerals dominated by weak first order cubic magnetocrystalline anisotropy with  $K_1 < 0$  have

Notes to Table 2: For each spectrum, we report effective  $g$ -factor ( $g_{\text{eff}}$ ), the peak-to-peak linewidth in the derivative spectrum ( $\Delta B$ ), and the asymmetry ratio  $A = \Delta B_{\text{high}}/\Delta B_{\text{low}}$ . See Fig. 2a for a graphical depiction of these parameters.

<sup>a</sup> These samples exhibited some FMR absorption at zero field, which complicates a precise characterization of  $\Delta B_{\text{low}}$  and, by implication,  $\Delta B_{\text{FWHM}}$  and  $A$ . To calculate  $\Delta B_{\text{low}}$  for these samples, we subtracted the zero-field absorption value in the derivative spectrum from all data points below  $B_{\text{eff}}$  prior to integrating the spectrum.

<sup>b</sup> These two samples exhibited extreme zero-field absorption; no method will accurately measure the low-field linewidth and shape of such samples. Instead, for these samples, we calculated  $\Delta B_{\text{low}}$  in the same way as for the samples with no zero-field absorption. This will give a lower limit for  $\Delta B_{\text{low}}$  and therefore a lower limit for  $\Delta B_{\text{FWHM}}$  and an upper limit for  $A$ .

<sup>c</sup> This sample exhibited a single strong resonance line at  $g_{\text{eff}} = 4.3$  and a sextet of resonance lines centered at  $g_{\text{eff}} = 2.0$  from paramagnetic  $\text{Fe}^{3+}$  and  $\text{Mn}^{2+}$ , respectively. This paramagnetic resonance effectively obscures any underlying ferromagnetic signal.

$g_{\text{eff}} > 2.12$ ,  $A > 1$ , and only very weak low-field absorption peaks (see Fig. 2 of [41]).

In fact, we know of no other published FMR spectra of stoichiometric magnetites which share any one of these properties, much less all three simultaneously (except for perhaps the report of “magnetite-like” phases with  $K_1 > 0$  in synthetic borosilicate glasses and simulated lunar glasses [41]). Other cubic minerals, like high-Ti magnetite ( $\text{Fe}_{3-x}\text{Ti}_x\text{O}_4$  with  $x > 0.55$ ), native iron, and cobalt-rich ferrites, have  $K_1 > 0$  such that  $A < 1$  and  $g_{\text{eff}} < 2$  [42–44]. However, our low-temperature data (Fig. 1b,c) as well as numerous previous studies [12] conclusively show that magnetosomes are composed of nearly stoichiometric magnetite. That magnetotactic bacteria do not fit this rule suggests that their internal fields are not dominated by magnetocrystalline anisotropy.

#### 4.2.2. Unusual FMR signature of magnetotactic bacteria

Clearly, magnetotactic bacteria must have some other strong source of magnetic anisotropy. This additional anisotropy is unlikely to be magnetoelastic because pure magnetite’s magnetoelastic anisotropy constant, although positive, is typically only  $\sim 20\%$  of  $|K_1|$  at room temperature [25]. Instead, we suggest that the unusual FMR spectra of magnetotactic bacteria results primarily from the alignment of the magnetosomes in chains. Because these magnetosomes are only separated by a few nm, they each should experience interaction fields approaching the orientation and intensity of that of a single, elongate SD crystal aligned in the same direction as the chain axis. In this approximation, magnetosome chains would be dominated by positive uniaxial shape anisotropy [25]. Previous data and modeling have shown that positive uniaxial materials have  $A < 1$ ,  $g_{\text{eff}} < 2.12$ , and can have low-field secondary absorption peaks if the anisotropy is sufficiently intense (see Supplementary Information).

Such a model is consistent with both previous electron holography studies of MS-1 [45,46], which show magnetic field lines being diverted away from the magnetocrystalline easy axis toward the magnetosome chain axis, and with hysteresis data [12], which show that magnetosome chains have saturation remanence to saturation magnetization ratios of  $\sim 0.5$ . However, note that this uniaxial model must be only an approximation, because (a) the magnetosome

chains are not single, elongate crystals, (b) magnetosome chains have much lower coercivities than acicular magnetite crystals with the same axial ratios [47], and (c) the four species have linewidths equal to that expected for cylinders with width-to-length ratios ranging between 0.2 to 0.5 (using  $\Delta B$  from Table 2, Eq. (2) from our Supplementary Materials, and Eq. (3) from [48]), somewhat larger than our actual magnetosome chain aspect ratios of  $\sim 0.05$ – $0.1$ . Related to the latter caveat, a single magnetite cylinder with an aspect ratio of 0.1 should achieve resonance at 500 mT (19 mT) when it is aligned perpendicular (parallel) to the applied field (using Eq. (1) of [38] and ellipsoid demagnetizing factors from [48]), whereas the FMR spectra of our magnetosome samples extend from only  $\sim 200$  to  $\sim 400$  mT. We note also that at least for MV-1 and MC-1 (but not for the equant crystals in AMB-1 and MS-1), the shape anisotropy of the *individual* magnetosome crystals (which have an axis of elongation coincident with the chain axis) could also contribute to the FMR asymmetry.

With these caveats, we propose, following [49–51], that it is the magnetosome chains’ uniaxial-like anisotropy that is responsible for their having  $A < 1$  and  $g_{\text{eff}} < 2.12$ . Following [50–52], we might also suggest that the chains’ low-field ripple structure is a reflection of the large absolute magnitude of the chain’s uniaxial-like anisotropy (see Supplementary Information). The detailed differences between the computed FMR spectra of truly uniaxial materials [50,51] and those of magnetotactic bacteria (Fig. 2) can be attributed to the fact that the latter are only approximately uniaxial. A more detailed description of the FMR properties expected for uniaxial materials can be found in the Supplementary Information.

This proposition should be confirmed with direct micromagnetic modeling of magnetosome chains, perhaps beginning with a chain of spheres approximation [47]. As an empirical test, we measured the FMR properties of the Lysed AMB-1 (Fig. 2e). The FMR spectrum was dramatically different than the whole cells, instead resembling that of the Chiton (Fig. 2i) and synthetic magnetites and maghemites (Fig. 2l–n). The increase in  $\Delta B$  and  $A$  after lysing is almost certainly a result of the strong, three-dimensional interactions resulting from the clumping of the magnetosomes following lysing. We also measured the FMR spectra of several powders of elongate maghe-

mite and magnetite crystals that should have uniaxial shape anisotropy. Again, like for Lysed AMB-1, the strong magnetostatic interactions in these samples controlled the spectra such that it is difficult to see the effects of the anisotropy fields of the individual crystals. Thus, we have not yet successfully measured the FMR properties of an isolated magnetosome nor an isolated crystal with uniaxial shape anisotropy. Nevertheless, the lysing experiment makes clear that the FMR spectra of magnetosomes are strongly influenced by the spatial positions of the crystals, such that chains (which contain one dimensional interactions along the chain axis) have a distinct signature from clumps (which have three-dimensional interactions).

Although we were unable to measure the FMR properties of non-interacting SD powders with uniaxial shape anisotropy, we did measure the FMR properties of weakly interacting SD crystallites that should be dominated by other forms of uniaxial anisotropy. For instance, natural hematites are almost always dominated by positive uniaxial magnetoelastic anisotropy, while concentrated powders of this mineral should not be dominated by interactions because hematite's  $M_s$  is only 3 mT [25]. Therefore, from Eq. (4) in our Supplementary Information, we might expect hematite powders to have  $\Delta B \sim$  several hundred mT and  $A < 1$  (for a magnetostriction of  $\lambda_s = 8 \times 10^{-6}$  and internal stress of  $\sigma = 10\text{--}100$  MPa as described in [25]). Indeed, our SD hematite powder exhibits a weak uniaxial spectrum with  $A \sim 0.7$  (Fig. 2q). A second example might be goethite, which should be dominated by positive uniaxial magnetocrystalline anisotropy [53], although the precise value of  $K_u$  is somewhat in dispute ( $+1\text{--}10 \times 10^5$  [54]). Two of our three goethite powders (Inorganic Goethite and Goethite TD) have  $A < 1$  (e.g., Fig. 2r), although their linewidths are much less broad than would be predicted by FMR theory. The third goethite sample (Goethite TD) has a broader linewidth and has  $A > 1$ ; the latter may be a result of the broadness of the linewidth (due to the fact that  $dI/dB$  is an odd function of  $B$ ; see Supplementary Information) rather than a lack of uniaxial anisotropy.

#### 4.2.3. FMR spectra of magnetites at 77 K

The 77 K spectra of all the SD and larger magnetite-bearing samples have larger  $g_{\text{eff}}$ ,  $\Delta B$ , and  $A$  than the room-temperature spectra. This includes the magnetotactic bacteria, for which the sense of spectral asym-

metry actually reverses (e.g.,  $A$  increases above 1) upon cooling to 77 K. We suggest that the changes in these parameters at 77 K are a reflection of magnetite's Verwey transition. At 77 K, magnetite will have monoclinic magnetocrystalline anisotropy with a hard axis energy  $> 2.5 \times 10^5 \text{ J m}^{-3}$  [27,55], which corresponds to a bulk coercivity  $H_c \sim 400$  mT and linewidth  $\Delta B_a \sim 1000$  mT (see Supplementary Information). This exceeds the  $H_c \sim 150$  mT and linewidth  $\Delta B_u \sim 500$  mT from the uniaxial shape anisotropy of elongate whisker magnetites at these temperatures and means that  $g_{\text{eff}}$  and  $\Delta B$  should increase below the Verwey transition for both shape-controlled as well as equant grains, as has been previously observed [56]. That monoclinic anisotropy has a good approximation an easy plane and therefore has an angular dependence very close to that of negative uniaxial anisotropy (compare Fig. 16 of [27] with Fig. 5.10 of [57]) can explain why  $A > 1$  for magnetite below the Verwey transition (see Supplementary Information).

## 5. Two rock magnetic tests for magnetosome chains

Our results demonstrate that magnetotactic bacteria have distinct rock magnetic properties by which they can be identified. There are now two techniques that can be used to rapidly identify them in bulk samples: the Moskowitz test and ferromagnetic resonance. Both apparently are sensitive to the arrangement of magnetite crystals in linear chains. Although neither technique provides as definitive an identification as TEM, both are much less time-consuming than TEM and are sensitive to very low concentrations of magnetotactic bacteria in samples. They are therefore potentially powerful tools for rapidly screening large quantities of sediments for magnetotactic bacteria and magnetofossils. Any bulk sample with magnetic properties characteristic of chains can always be targeted with TEM for conclusive verification of the presence of magnetofossils. This may permit wide-ranging searches for magnetofossils in natural sediments.

### 5.1. Application to magnetofossil-bearing carbonates

As a sensitivity test, we measured the FMR absorption of three carbonate samples containing mag-

netofossil chains confirmed by previous TEM and ARM studies. Their FMR spectra showed a sextet of narrow, paramagnetic resonance lines centered at 33 mT ( $g_{\text{eff}}=2.0$ ) characteristic of  $\text{Mn}^{2+}$  in carbonate, superimposed on a broad, intense background absorption which we ascribe to the magnetite in these samples. The background absorption of one of the three samples—Clino 985'0"—has  $A < 1$  and also has secondary absorption peaks on the low-field side of the peak absorption. The other two Clino samples had nearly symmetric lineshapes ( $A \sim 1.0$ ). It is clear from the relatively narrow and symmetric lineshape centered near  $g=2.12$  that FMR successfully detected the presence of the fine-grained SD magnetites in all three samples. Furthermore, if the extended low-field absorption and secondary low-field peak in the Clino 985'0" spectrum is also from magnetite, then FMR also successfully identified magnetosome chains in Clino 985'0".

The Moskowitz test was not able to detect magnetofossils in any of the three Clino samples nor on previously studied marine carbonate samples. In fact, we know of no published study in which the Moskowitz test has conclusively identified magnetofossil chains (e.g., found  $\delta_{\text{FC}}/\delta_{\text{ZFC}} > 2$ ) in natural sediments [34,37,58,59]. This failure is at least partly the result of from the fact that the Verwey transition is easily suppressed in fine-grained magnetites after even slight surface oxidation that readily occurs in air at room temperature. A second difficulty is that the Verwey transition and the  $\delta_{\text{FC}}/\delta_{\text{ZFC}}$  ratio are also suppressed when magnetosome chains are mixed with other magnetites like non-SD magnetites, SD magnetites not in chains, and other ferromagnetic minerals [8]. The latter is exemplified by the Clino 993'1" sample, in which SP magnetites (that are responsible for the rise with decreasing temperature in their FC and ZFC moments) are "washing out" the Verwey transition at  $\sim 112$  K.

### 5.2. Comparison of Moskowitz and FMR tests

From this perspective, FMR has several distinct advantages as a magnetofossil detector over the Moskowitz test. As demonstrated by its detection of the fine-grained magnetite in the Old MS-1 and the Clino samples, FMR is still sensitive to magnetosome chains which have surface oxidation rinds that

make them otherwise undetectable with the Moskowitz test. Since all but the youngest magnetofossil chains tend to be maghemitized, this is a major advantage.

This points to another advantage: FMR should be able to identify chains of SD grains of a wide variety of minerals other than just magnetite. Any SD ferromagnetic mineral that is dominated by shape anisotropy for most aspect ratios would presumably have a much different FMR signature when arranged in linear chains (for which the FMR spectrum would have  $A < 1$  and possibly secondary absorption peaks) than when not in chains (for which  $A$  would be larger and could even exceed 1 depending on the anisotropy of the individual magnetosomes). Although only magnetite-bearing magnetosomes have been identified so far in the fossil record (with the possible exception of [60]), it is certain that bacteria with magnetosomes made of greigite [61], or perhaps a diversity of other minerals, should be leaving fossils behind as well.

With a moment sensitivity of about  $10^{11}$  to  $10^{15}$  electron spins ( $10^{-12}$  to  $10^{-8}$  A m<sup>2</sup>) [62], FMR spectrometers are comparable to that of the most sensitive low-temperature susceptometers like our superconducting MPMS (which has a sensitivity of  $\sim 10^{-9}$  to  $10^{-10}$  A m<sup>2</sup>) and superior compared to the more common vibrating sample magnetometers (which have sensitivities of  $\sim 10^{-9}$  to  $10^{-8}$  A m<sup>2</sup>). A recent study of marine carbonates [31] found that compared to the vibrating sample magnetometers, FMR could detect 100 times smaller concentrations of ferrimagnetic minerals and 105 times smaller concentrations of paramagnetic minerals.

Both the Moskowitz and FMR tests are less sensitive to magnetosome chains that are not in pure culture but rather mixed with a population of non-chain ferromagnetic crystals. Simulations by Moskowitz et al. [8] have shown that when chains are mixed with a volume fraction of only about >10% non-chain SD magnetites, >20% non-chain SP magnetites, or >30% non-chain MD magnetites, the  $\delta_{\text{FC}}/\delta_{\text{ZFC}}$  ratio of the assemblage is depressed below 2. The Moskowitz test would not definitively identify magnetofossil chains in mixed assemblages with non-chain magnetites above these abundances. We have conducted similar simulations to assess the sensitivity of FMR to mixed assemblages of chains and non-chain mag-

netites (Fig. 4). Because the FMR spectrum of a randomly oriented polycrystalline assemblage is a superposition of the FMR spectra of all the individual crystallites (assuming no magnetostatic interactions) [41,44,52], it is straightforward to calculate the FMR spectrum of an assemblage of non-chain crystals with isolated chains using a linear mixing model. Prior to the summation, the spectra of each of the two end members are weighted according to their relative volume fraction in the assemblage. The results (Fig. 4) show that when magnetotactic bacteria are mixed with more than a few tens of percent (by weight or mass) non-chain magnetites,  $A$  rises above unity,  $g_{\text{eff}}$  increases above 2.12, and the secondary absorption peaks at fields between  $\sim 200$  and  $300$  mT disappear. This makes it moderately more effective than the Moskowitz test, which requires 70–90% of such an assemblage to be in chains.

With acquisition times of just 5–10 min, room-temperature FMR spectra are much faster to acquire than the low-temperature data for the Moskowitz test, which require at least several hours. Also, because they do not operate at liquid He temperatures, typical FMR spectrometers are much cheaper to operate than the MPMS used for the Moskowitz test. On the other hand, because the Moskowitz test senses the Verwey transition, it can readily distinguish magnetite from other ferromagnetic minerals that might have room-temperature FMR spectra similar to magnetosome chains.

For instance, SD assemblages of minerals with positive uniaxial magnetocrystalline anisotropy like goethite (dominated by magnetocrystalline anisotropy), hematite (dominated by magnetoelastic anisotropy), and cubic minerals with  $K_1 > 0$  like high-Ti magnetite also could have  $A < 1$ . Goethite and hema-

tite in particular might complicate searches for ancient magnetofossils in weathered sediments, although the very weak magnetism of these phases

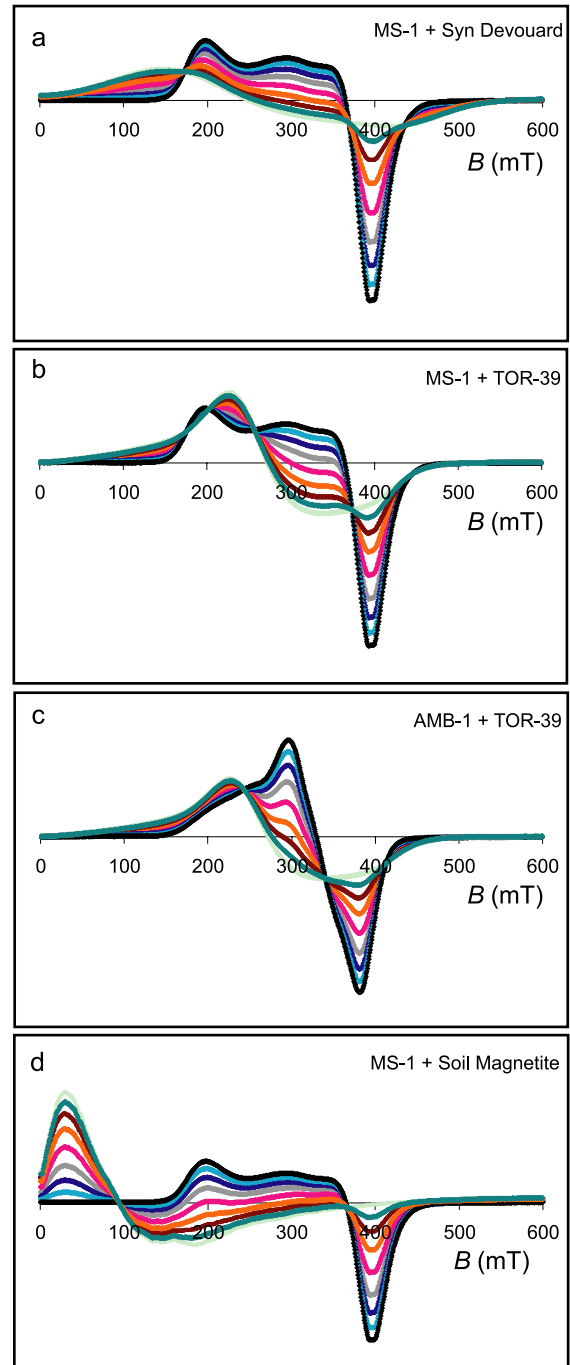


Fig. 4. Simulated FMR spectra of assemblages of magnetotactic bacteria (isolated magnetite chains) with non-chain magnetites. These were computed using a linear mixing model in which end member spectra from Fig. 2 were weighted according to the specified chain mass fraction in the assemblage: 100% magnetosome chains (black spectra), 91% chains (light blue spectra), 80% chains (dark blue spectra), 66% chains (grey spectra), 50% chains (pink spectra), 33% chains (orange spectra), 25% chains (brown spectra), 9% chains (dark green spectra), 0% chains (light green spectra). (a) MS-1 mixed with Syn Devouard, (b) MS-1 mixed with TOR-39, (c) AMB-1 mixed with TOR-39, (d) MS-1 mixed with Soil magnetite.

means that even small amounts of admixed magnetite would dominate the FMR spectra. Fortunately, the most commonly found alteration product of magnetofossils, maghemite, should not easily be mistaken for chains because SD maghemite has negative  $K_1$  [25] (and so should have  $A > 1$ ). Also, our measurements on the oxidized magnetosome chains (Old MS-1) suggest that partly maghemitized magnetosomes may retain the characteristic  $A < 1$  signature identified for unaltered chains. In any case, these and most other “doppelgänger” minerals could still be easily distinguished from magnetosomes by taking FMR spectra in a continuous range of temperatures spanning the Verwey transition, across which the line shape and width would change discontinuously if magnetite were present [40]. Unfortunately, variable temperature FMR could not help in distinguishing magnetosome chains from elongate magnetites. This may be of concern because average rock magnetite has an elongation of 1.5:1 [25] and is dominated by positive uniaxial shape anisotropy). On the other hand, the latter axial ratios are 10–100 times less than that of typical chains and, more importantly, their average size is in the PSD range; these two factors at least partly explain why our Kilauea basalt sample does not have a magnetotactic bacteria-like spectrum. In the end, we expect the most significant hindrance to using FMR as a magnetofossil detector will likely not be other ferromagnets but the overprinting of the FMR signal by resonance from common paramagnets like  $Mn^{2+}$  or  $Fe^{3+}$  (as demonstrated in Fig. 2h,o).

## 6. Conclusions

1. The Moskowitz test uniquely identifies magnetotactic bacteria with intact chains, including the previously unmeasured bacterium AMB-1.
2. We provide experimental evidence that the Moskowitz test accomplishes this at least in part due to its sensitivity to the bacteria’s magnetosome chain structure.
3. Four species of magnetotactic bacteria have FMR spectra distinct from all other samples in our study.
4. We suggest that their unique spectra result from the magnetosome chain structure which effectively imparts a positive uniaxial anisotropy on each magnetosome.
5. Even partly oxidized magnetosome chains that are not detectable with the Moskowitz test can retain the FMR signature distinctive of pristine magnetotactic bacteria.
6. FMR may be a powerful tool for rapidly identifying magnetofossils of a wide variety of mineralogies in bulk sediments.

## Acknowledgements

We thank H. Vali, Y. Roh, B. Bertani, D. Newman, M. Dubiel, B. Moskowitz, D. Lovley, G. Rossman, and A. Kappler for providing many of the samples used in this study. We also thank T. Bosak for comments on an earlier draft of this manuscript, and D. Griscom and B. Moskowitz for their thoughtful reviews. S.S.K. was supported by the Mars Instrument Development Project Program, A.K. by a Beckman Senior Research Fellowship, R.E.K. by an NSF Graduate Research Fellowship, and J.L.K. and B.P.W. by the NASA Exobiology Program and the NASA Astrobiology Institute. *[KF]*

## References

- [1] S.-B.R. Chang, J.L. Kirschvink, Magnetofossils, the magnetization of sediments, and the evolution of magnetite biomineralization, *Annu. Rev. Earth Planet. Sci.* 17 (1989) 169–195.
- [2] M. Seufferheld, M.C.F. Vieira, F.A. Ruiz, C.O. Rodrigues, S.N.J. Moreno, R. Docampo, Identification of organelles in bacteria similar to acidocalcisomes of unicellular eukaryotes, *J. Biol. Chem.* 278 (2003) 29971–29978.
- [3] J.L. Kirschvink, J.W. Hagadorn, A grand unified theory of biomineralization, in: E. Bäuerlein (Ed.), *Biomineralization*, Wiley-VCH Verlag, Weinheim, Germany, 2000, pp. 139–140.
- [4] I.E. Friedmann, J. Wierzbos, C. Ascaso, M. Winklhofer, Chains of magnetite crystals in the meteorite ALH84001: evidence of biological origin, *Proc. Natl. Acad. Sci. U. S. A.* 98 (2001) 2176–2181.
- [5] K.L. Thomas-Keptra, S.J. Clemett, D.A. Bazylinski, J.L. Kirschvink, D.S. McKay, S.J. Wentworth, H. Vali, E.K. Gibson, C.S. Romanek, Magnetofossils from ancient Mars: a robust biosignature in the martian meteorite ALH84001, *Appl. Environ. Microbiol.* 68 (2002) 3663–3672.
- [6] K.L. Thomas-Keptra, D.A. Bazylinski, J.L. Kirschvink, S.J. Clemett, D.S. McKay, S.J. Wentworth, H. Vali, E.K. Gibson Jr., C.S. Romanek, Elongated prismatic magnetite crystals in ALH84001 carbonate globules: potential Martian magnetofossils, *Geochim. Cosmochim. Acta* 64 (2000) 4049–4081.

- [7] K.L. Thomas-Keppta, S.J. Clemett, D.A. Bazylinski, J.L. Kirschvink, D.S. McKay, W.S.J.H. Vali, E.K.J. Gibson, M.F. McKay, C.S. Romanek, Truncated hexa-octahedral magnetite crystals in ALH84001: presumptive biosignatures, *Proc. Natl. Acad. Sci. U. S. A.* 98 (2001) 2164–2169.
- [8] B.M. Moskowitz, R.B. Frankel, D.A. Bazylinski, Rock magnetic criteria for the detection of biogenic magnetite, *Earth Planet. Sci. Lett.* 120 (1993) 283–300.
- [9] B. Carter-Stiglitz, M. Jackson, B. Moskowitz, Low-temperature remanence in stable single domain magnetite, *Geophys. Res. Lett.* 29 (2002) DOI: 10.1029/2001GL014197.
- [10] H.A. Lowenstam, Minerals made by organisms, *Science* 211 (1981) 1126–1131.
- [11] J.L. Kirschvink, H.A. Lowenstam, Mineralization and magnetization of chiton teeth: paleomagnetic, sedimentologic, and biologic implications of organic magnetite, *Earth Planet. Sci. Lett.* 44 (1979) 193–204.
- [12] D.A. Bazylinski, B.M. Moskowitz, Microbial biomineralization of magnetic iron minerals: microbiology, magnetism, and environmental significance, in: J.F. Bandfield, K.H. Nealson (Eds.), *Geomicrobiology: Interactions between Microbes and Minerals*, Mineralogical Society of America, Washington, DC, 1997, pp. 181–223.
- [13] T. Matsunaga, T. Sakaguchi, Production of biogenic magnetite by aerobic magnetic spirilla strains AMB-1 and MGT-1, in: T. Matsunaga (Ed.), *Ferrites: Proceedings of the Sixth International Conference on Ferrites*, Japan Society of Powder and Powder Metallurgy, Tokyo, 1992, pp. 262–267.
- [14] D.F. McNeill, G.P. Eberli, B.H. Lidz, P.K. Swart, J.A.M. Kenter, Chronostratigraphy of a prograded carbonate platform margin: a record of dynamic slope sedimentation, Western Great Bahama Bank, *Subsurface Geology of a Prograding Carbonate Platform Margin, Great Bahama Bank: Results of the Bahamas Drilling Project*, SEPM Special Publication, vol. 70, 2001, pp. 101–134.
- [15] D.F. McNeill, J.L. Kirschvink, Early dolomitization of platform carbonates and the preservation of magnetic polarity, *J. Geophys. Res.* 98 (1993) 7977–7986.
- [16] N.H.C. Sparks, S. Mann, D.A. Bazylinski, D.R. Lovley, H.W. Jannasch, R.B. Frankel, Structure and morphology of magnetite anaerobically-produced by a marine magnetotactic bacterium and a dissimilatory iron-reducing bacterium, *Earth Planet. Sci. Lett.* 98 (1990) 14–22.
- [17] R.D. Stapleton, Z.L. Sabree, A.V. Palumbo, C. Moyer, A. Devol, Y. Roh J.-Z. Zhou, Metal reduction at in situ temperatures by *Shewanella* isolates from diverse marine environments, *Aquat. Microb. Ecol.* (submitted for publication).
- [18] C.L. Zhang, H. Vali, C.S. Romanek, T.J. Phelps, S.V. Liu, Formation of single-domain magnetite by a thermophilic bacterium, *Am. Mineral.* 83 (1998) 1409–1418.
- [19] Y. Roh, S.V. Li, G. Li, H. Huang, T.J. Phelps, J. Zhou, Isolation and characterization of metal-reducing *Thermoanaerobacter* strains from deep subsurface environments of the Piceance Basin, Colorado, *Appl. Environ. Microbiol.* 68 (2002) 6013–6020.
- [20] K. Kashefi, D.R. Lovley, Reduction of Fe(III), Mn(IV), and toxic metals at 100 degrees C by *Pyrobaculum islandicum*, *Appl. Environ. Microbiol.* 66 (2000) 1050–1056.
- [21] B. Devouard, M. Posfai, X. Hua, D.A. Bazylinski, R.B. Frankel, P.R. Buseck, Magnetite from magnetotactic bacteria: size distributions and twinning, *Am. Mineral.* 83 (1998) 1387–1398.
- [22] M. Kiyama, Production of fine particles by wet methods, *Ceram. Data*, (1983) 137–142 (Kyoto Seihin Gijutsu Kyokai).
- [23] S.L. Halgedahl, R. Jarrard, Low-temperature behavior of single-domain through multidomain magnetite, *Earth Planet. Sci. Lett.* 130 (1995) 127–139.
- [24] J.W. Holt, J.L. Kirschvink, Geomagnetic field inclinations for the past 400 kyr from the 1-km core of the Hawaii Scientific Drilling Project, *J. Geophys. Res.* 101 (1996) 11655–11663.
- [25] D.J. Dunlop, O. Ozdemir, *Rock Magnetism: Fundamentals and Frontiers*, Cambridge Univ. Press, New York, 1997, 573 pp.
- [26] L. Tauxe, H.N. Bertram, C. Seberino, Physical interpretation of hysteresis loops: micromagnetic modeling of fine particle magnetite, *Geochem. Geophys. Geosystems* 3 (2002) DOI: 10.1029/2001GC000241.
- [27] A.R. Muxworthy, E. McClelland, Review of the low-temperature magnetic properties of magnetite from a rock magnetic perspective, *Geophys. J. Int.* 140 (2000) 101–114.
- [28] V.A.M. Brabers, F. Walz, H. Kronmuller, Impurity effects upon the Verwey transition in magnetite, *Phys. Rev., B* 58 (1998) 14163–14166.
- [29] F. Walz, J.H.V.J. Brabers, V.A.M. Brabers, The Verwey transition in magnetite as studied by means of definite impurity doping, *Z. Met.kd.* 93 (2002) 1095–1102.
- [30] B. Carter-Stiglitz, B. Moskowitz, M. Jackson, More on the low-temperature magnetism of stable single domain magnetite: reversibility and nonstoichiometry, *Geophys. Res. Lett.* 31 (2004) DOI: 10.1029/2003GL019155.
- [31] N.P. Crook, S.R. Hoon, K.G. Taylor, C.T. Perry, Electron spin resonance as a high sensitivity technique for environmental magnetism: determination in carbonate sediments, *Geophys. J. Int.* 149 (2002) 328–337.
- [32] B. Carter-Stiglitz, B. Moskowitz, M. Jackson, Correction to “Low-temperature remanence in stable single domain magnetite” (vol 29, pg 7, 2002), *Geophys. Res. Lett.* 30 (2003) DOI: 10.1029/2003GL018727.
- [33] J.L. Kirschvink, Microwave absorption by magnetite: a possible mechanism for coupling nonthermal levels of radiation to biological systems, *Bioelectromagnetics* 17 (1996) 187–194.
- [34] A. Smirnov, J.A. Tarduno, Low-temperature magnetic properties of pelagic sediments (Ocean Drilling Program Site 805C): tracers of maghemitization and magnetic mineral reduction, *J. Geophys. Res.* 105 (2000) 16457–16471.
- [35] A. Kosterov, Low-temperature magnetic hysteresis properties of partially oxidized magnetite, *Geophys. J. Int.* 149 (2002) 796–804.
- [36] The Rock Magnetic Bestiary, <http://www.geo.umn.edu/orgs/irm/bestiary/index.html> (2003).
- [37] H.F. Passier, M.J. Dekkers, Iron oxide formation in the active oxidation front above sapropel S1 in the eastern Mediterranean Sea as derived from low-temperature magnetism, *Geophys. J. Int.* 150 (2002) 230–240.

- [38] D.L. Griscom, C.L. Marquardt, E.J. Friebale, D.J. Dunlop, Magnetic hysteresis in the F.M.R. spectra of fine-grained spherical iron: possible evidence for a new carrier of hard remanence in lunar rocks and soils, *Earth Planet. Sci. Lett.* 24 (1974) 78–85.
- [39] G. Calas, Electron paramagnetic resonance, in: F.C. Hawthorne (Ed.), *Spectroscopic Methods in Mineralogy and Geology*, Reviews in Mineralogy, vol. 18, Mineralogical Association of America, Chelsea, 1988, pp. 513–571.
- [40] D.L. Griscom, V. Beltran-Lopez, C.I. Merzbacher, E. Bolden, Electron spin resonance of 65-million-year-old glasses and rocks from the Cretaceous–Tertiary boundary, *J. Non-Cryst. Solids* 253 (1999) 1–22.
- [41] D.L. Griscom, Ferromagnetic resonance of precipitated phases in natural glasses, *J. Non-Cryst. Solids* 67 (1984) 81–118.
- [42] J.E. Pippin, C.L. Hogan, Resonance measurements on nickel–cobalt ferrites as a function of temperature and nickel ferrite-aluminates, *IRE Trans. MTT* 6 (1958) 77–82.
- [43] P.J.B. Clarricoats, *Microwave Ferrites*, Wiley, New York, 1961.
- [44] D.L. Griscom, Ferromagnetic resonance spectra of lunar fines: some implications of line shape analysis, *Geochim. Cosmochim. Acta* 38 (1974) 1509–1519.
- [45] R.E. Dunin-Borkowski, M.R. McCartney, M. Posfai, R.B. Frankel, D.A. Bazylinski, P.R. Buseck, Off-axis electron holography of magnetotactic bacteria: magnetic microstructure of strains MV-1 and MS-1, *Eur. J. Mineral.* 13 (2001) 671–684.
- [46] R.E. Dunin-Borkowski, M.R. McCartney, R.B. Frankel, D.A. Bazylinski, M. Posfai, P.R. Buseck, Magnetic microstructure of magnetotactic bacteria by electron holography, *Science* 282 (1998) 1868–1870.
- [47] B. Moskowitz, R. Frankel, P. Flanders, R. Blakemore, B. Schwartz, Magnetic properties of magnetotactic bacteria, *J. Magn. Magn. Mater.* 73 (1988) 273–288.
- [48] R.I. Joseph, Demagnetizing factors in nonellipsoidal samples—a review, *Geophysics* 41 (1976) 1052–1054.
- [49] C.A. Morrison, N. Karayianis, Ferromagnetic resonance in uniaxial polycrystalline materials, *J. Appl. Phys.* 29 (1958) 339–340.
- [50] C. Surig, K.A. Hempel, F. Schumacher, Microwave absorption in singledomain particles involving first- and second-order uniaxial magnetic anisotropy constant, *J. Magn. Magn. Mater.* 117 (1992) 441–447.
- [51] C. Surig, K.A. Hempel, R.A. Muller, P. Gornert, Investigations on  $Zn_{2-x}Co_xW$ -type hexaferrites powders at low temperatures by ferromagnetic resonance, *J. Magn. Magn. Mater.* 150 (1995) 270–276.
- [52] E. Schlomann, R.V. Jones, Ferromagnetic resonance in polycrystalline ferrites with hexagonal crystal structure, *J. Appl. Phys.* 30 (1959) 177S–178S.
- [53] M.J. Dekkers, Magnetic properties of natural goethite: I. Grain-size dependence of some low- and high-field related rock-magnetic parameters measured at room temperature, *Geophys. J.* 97 (1989) 323–340.
- [54] Q.A. Pankhurst, The magnetism of fine particle iron oxides and oxyhydroxides in applied fields, *Hyperfine Interact.* 90 (1994) 201–214.
- [55] K. Abe, Y. Miyamoto, S. Chikazumi, Magnetocrystalline anisotropy of low temperature phase of magnetite, *J. Phys. Soc. Jpn.* 41 (1976) 1894–1902.
- [56] V.N. Sharma, The  $g$  factor of polycrystalline magnetite at low temperature, *J. Appl. Phys.* 36 (1965) 1450–1452.
- [57] G. Bertotti, *Hysteresis in Magnetism: For Physicists, Materials Scientists, and Engineers*, Academic Press, San Diego, 1998, 558 pp.
- [58] S.A. Brachfeld, S.K. Banerjee, Y. Guyodo, G.D. Acton, A 13200 year history of century to millennial-scale paleoenvironmental change magnetically recorded in the Palmer Deep, western Antarctic Peninsula, *Earth Planet. Sci. Lett.* 194 (2002) 311–326.
- [59] C.E. Geiss, S.K. Banerjee, A multi-parameter rock magnetic record of the last glacial–interglacial paleoclimate from south-central Illinois, USA, *Earth Planet. Sci. Lett.* 152 (1997) 203–216.
- [60] A. Demitrac, A search for bacterial magnetite in the sediments of Eel Marsh, Woods Hole, Massachusetts, in: J.L. Kirschvink, D.S. Jones, B.J. MacFadden (Eds.), *Magnetite Biomineralization and Magnetoreception in Organisms: A New Biomagnetism*, vol. 5, Plenum, New York, 1985, pp. 625–644.
- [61] M. Posfai, P.R. Buseck, D.A. Bazylinski, R.B. Frankel, Iron sulfides from magnetotactic bacteria: structure composition, and phase transitions, *Am. Mineral.* 83 (1998) 1469–1481.
- [62] A.B. Vassilikou-Dova, G. Lehmann, Investigations of minerals by electron paramagnetic resonance, *Fortschr. Mineral.* 65 (1987) 173–202.